

University of Groningen

## Deciphering the Chemical Basis of Fluorescence of a Selenium-Labeled Uracil Probe when Bound at the Bacterial Ribosomal A-Site

Cardenas, Gustavo; Menger, Maximilian F.S.J.; Ramos-Berdullas, Nicolás; Sánchez-Murcia, Pedro A.

*Published in:*  
Chemistry - A European Journal

*DOI:*  
[10.1002/chem.202004818](https://doi.org/10.1002/chem.202004818)

**IMPORTANT NOTE: You are advised to consult the publisher's version (publisher's PDF) if you wish to cite from it. Please check the document version below.**

*Document Version*  
Publisher's PDF, also known as Version of record

*Publication date:*  
2021

[Link to publication in University of Groningen/UMCG research database](#)

*Citation for published version (APA):*

Cardenas, G., Menger, M. F. S. J., Ramos-Berdullas, N., & Sánchez-Murcia, P. A. (2021). Deciphering the Chemical Basis of Fluorescence of a Selenium-Labeled Uracil Probe when Bound at the Bacterial Ribosomal A-Site. *Chemistry - A European Journal*, 27(15), 4927-4931.  
<https://doi.org/10.1002/chem.202004818>

### Copyright

Other than for strictly personal use, it is not permitted to download or to forward/distribute the text or part of it without the consent of the author(s) and/or copyright holder(s), unless the work is under an open content license (like Creative Commons).

The publication may also be distributed here under the terms of Article 25fa of the Dutch Copyright Act, indicated by the "Taverne" license. More information can be found on the University of Groningen website: <https://www.rug.nl/library/open-access/self-archiving-pure/taverne-amendment>.

### Take-down policy

If you believe that this document breaches copyright please contact us providing details, and we will remove access to the work immediately and investigate your claim.

Downloaded from the University of Groningen/UMCG research database (Pure): <http://www.rug.nl/research/portal>. For technical reasons the number of authors shown on this cover page is limited to 10 maximum.

## Fluorescence Probes

# Deciphering the Chemical Basis of Fluorescence of a Selenium-Labeled Uracil Probe when Bound at the Bacterial Ribosomal A-Site

Gustavo Cardenas,<sup>[a]</sup> Maximilian F. S. J. Menger,<sup>[b]</sup> Nicolás Ramos-Berdullas,<sup>[c]</sup> and Pedro A. Sánchez-Murcia<sup>\*[d, e]</sup>

**Abstract:** We unveil in this work the main factors that govern the turn-on/off fluorescence of a Se-modified uracil probe at the ribosomal RNA A-site. Whereas the constraint into an “in-plane” conformation of the two rings of the fluorophore is the main driver for the observed turn-on fluorescence emission in the presence of the antibiotic paromomycin, the electrostatics of the environment plays a minor role

during the emission process. Our computational strategy clearly indicates that, in the absence of paromomycin, the probe prefers conformations that show a dark  $S_1$  electronic state with participation of  $n\pi^*$  electronic transition contributions between the selenium atom and the  $\pi$ -system of the uracil moiety.

## Introduction

The fight against bacteria that are resistant to the existing antibiotic arsenal is one of the most crucial current challenges of humankind.<sup>[1–3]</sup> Amongst the different therapeutic approaches, some of these antibiotics target the ribosomal RNA decoding site (termed rRNA A-site) compromising the outcome of the protein biosynthesis machinery.<sup>[4,5]</sup> This process, the bacterial protein translation, presents a complex network of interactions. Thus, the implementation of smart chemical tools<sup>[6]</sup> to monitor its functional and temporal status—like environment-sensitive fluorescence probes<sup>[7–11]</sup>—is of great interest for the under-

standing of bacterial protein translation, and more importantly, can help in the design of a new generation of antibiotics that overcome resistance.<sup>[12]</sup> With this spirit, the selenium-modified responsive fluorescent ribonucleoside probe <sup>Se</sup>U (Scheme 1)<sup>[13]</sup> has proven to sense the presence of the antibiotic paromomycin (PAR) after incorporation into an oligonucleotide of the

[a] G. Cardenas

Chemistry Department, Universidad Autónoma de Madrid  
Calle Francisco Tomás y Valiente 7, 28049 Madrid (Spain)

[b] Dr. M. F. S. J. Menger

Zernike Institute for Advanced Materials  
Faculty of Science and Engineering, University of Groningen  
Nijenborgh 4, 9747 AG Groningen (The Netherlands)

[c] Dr. N. Ramos-Berdullas


Department of Physical Chemistry, University of Vigo  
Lagoas Marcosende s/n, 36310, Vigo (Spain)


[d] Dr. P. A. Sánchez-Murcia

Institute of Theoretical Chemistry  
Faculty of Chemistry, University of Vienna  
Währinger Straße 17, 1090 Vienna (Austria)

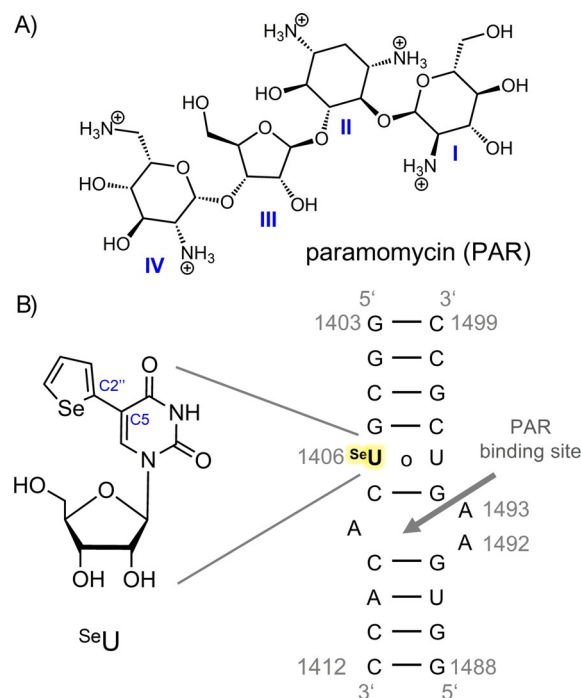
[e] Dr. P. A. Sánchez-Murcia

Present address:  
Division of Physiological Chemistry  
Otto-Loewi Research Center, Medical University of Graz  
Neue Stiftingstalstraße 6/III, 8010 Graz (Austria)  
E-mail: pedro.murcia@medunigraz.at

 Supporting information and the ORCID identification numbers for the

 authors of this article can be found under:

<https://doi.org/10.1002/chem.202004818>.



**Scheme 1.** A) Chemical structure of paromomycin (PAR); the four rings I–IV are labeled. B) Chemical structure of the nucleoside <sup>Se</sup>U and sequence of the rRNA model mimicking the A-site where <sup>Se</sup>U has been incorporated and studied.<sup>[14]</sup>

rRNA A-site, by leading to an increase of its fluorescence emission (aka. turn-on effect) in titration experiments.<sup>[14]</sup> The binding of PAR to bacterial rRNA<sup>[15,16]</sup> or to a small rRNA model<sup>[17,18]</sup> has been characterized in the past. Upon binding antibiotics of the aminoglycosides family,<sup>[19]</sup> adenine A1493 flips out (Figure 1).<sup>[17,20]</sup> To date, no structure is available of PAR bound to the <sup>Se</sup>U-modified rRNA. In principle, the extra selenophene ring in <sup>Se</sup>U (compared to a plain uracil) may affect the binding of PAR, and the other way around, PAR may affect the orientation of the fluorophore, and thereby, its fluorescence. A structure of a double-stranded rRNA incorporating <sup>Se</sup>U in position 1409,<sup>[14]</sup> shows two copies in the unit cell with different orientations for the nucleobase adenine 1493 (A1493) in the rRNA: flipped-out (chain A) and pointing to the major groove (chain B). The orientation of A1493 resembles the one found in the presence of PAR in the native rRNA<sup>[17]</sup> and might represent the physiological situation where the antibiotic is present.<sup>[14]</sup>

Due to the lack of structure of PAR bound to <sup>Se</sup>U-modified rRNA still many molecular and electronic features of the system stay unclear. Specially the fluorescence turn-on effect of the probe in the presence of the drug. Previous studies of <sup>Se</sup>U in solution showed that the probe was sensitive to changes of both polarity and viscosity of the solvent.<sup>[13]</sup> However, in the context of rRNA and PAR, it is still unknown what is it that determines the emission efficiency of the probe: the interactions with its environment or conformational changes in the probe as a consequence of the presence of PAR (or both)? In this work, we face these questions. We have used a compendium of modern classical and quantum mechanical methods to explain, first, the binding mode of PAR at the Se-modified RNA

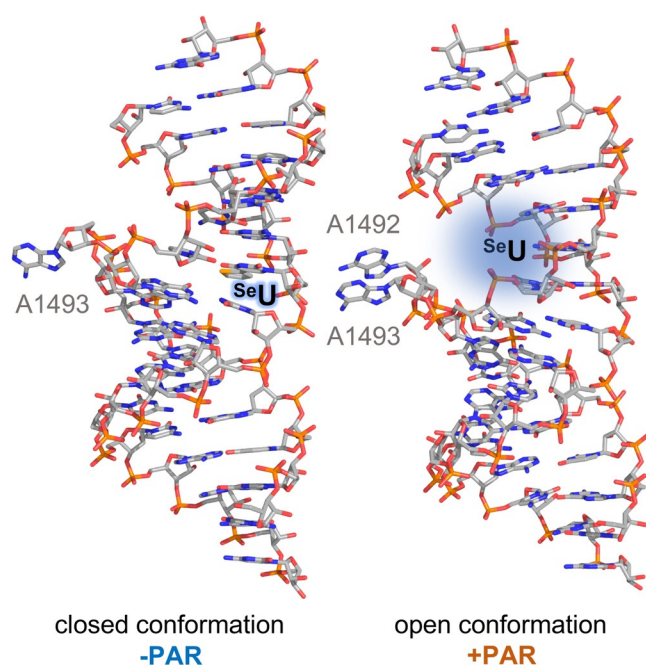


**Figure 1.** Flipped-in (closed conformation, chains A and B) and flipped-out (open conformation, chains C and D) conformations of a short rRNA structure modified with <sup>Se</sup>U (PDB ID: 5T3K).<sup>[14]</sup> These two conformations may correspond to the absence and presence of PAR, respectively.

A-site, and second, the turn-on effect of the fluorescence in <sup>Se</sup>U that is observed due to the presence of PAR at the A-site. With our approach we find that although there are no strong interactions between PAR and the Se-based probe <sup>Se</sup>U, the fluorescence of the latter drastically decreases because of conformational change leading to a disconnection between the  $\pi$ -system of the selenophene ring and the  $\pi$ -system of the uracil moiety in <sup>Se</sup>U if the antibiotic is absent.

## Results and Discussion

### Exploring the conformational space of <sup>Se</sup>U

In order to explore the binding mode of PAR into the rRNA site A, we simulated a ribosomal oligonucleotide containing the modified uracil <sup>Se</sup>U in the presence (+ PAR) and in the absence (− PAR) of paromomycin (Figure 2 and Section S1 in the Supporting Information). The Cartesian coordinates of the rRNA were taken from the solved structure deposited by Srivatsan and co-workers<sup>[14]</sup> shown in Figure 1. The antibiotic PAR was placed by superimposition with the crystal structure of native rRNA.<sup>[17]</sup> Each of the systems was equilibrated using classical MD simulations for a total time of 0.45  $\mu$ s ( $3 \times 0.15 \mu$ s) at 293 K. The temperature was chosen to match the temperature used in the experimental acquisition of the emission spectra. We kept the phosphate backbone constrained during the simulations with a small harmonic force on the phosphorous atoms ( $5 \text{ kcal mol}^{-1} \text{ \AA}^{-2}$ ) in order to preserve the RNA tertiary structure. As an outcome, we found that in the presence of PAR, the conformation of <sup>Se</sup>U does not change along the MD simulation, keeping a root-mean-squared distance (RMSD)

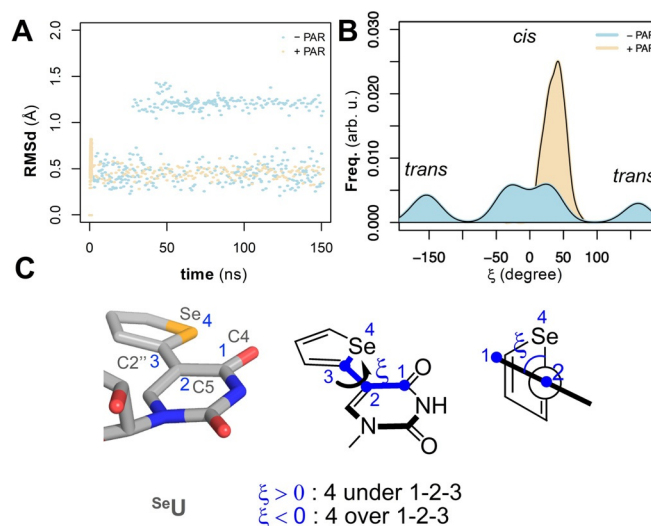


**Figure 2.** MD simulation of <sup>Se</sup>U-modified dsRNA containing <sup>Se</sup>U in the presence (+ PAR, orange dots and surfaces) and absence (− PAR, blue dots and surfaces) of paromomycin. A) RMSD [Å] evolution of <sup>Se</sup>U along MD simulations. B) Distribution of the dihedral angle  $\xi$  defined between C4–C5–C2′–Se atoms for 0.45  $\mu$ s time of MD simulation of − PAR and + PAR systems. The regions for *trans* and *cis* conformations are highlighted. C) Definition of dihedral angle  $\xi$  in two and three dimensions. A representative conformation of <sup>Se</sup>U is shown as sticks to highlight the atoms involved.

value under 0.5 Å (orange points, Figure 2A). In contrast, in the absence of the antibiotic, we observe two clusters of conformers for <sup>5e</sup>U (–PAR, blue points, Figure 2A). These clusters correspond to two different relative orientations of selenophene and uracil rings in <sup>5e</sup>U (Figure 2B and 2C). In the absence of PAR, the involved rotation around the bond C2'–C5 is allowed. This can be quantified by the measurement of the dihedral angle  $\xi$  defined between the two set of atoms C5–C4 and C2'–Se. In this way, if the value of  $\xi$  is close to 0°, the Se atom points towards the same side of oxygen O4 of the uracil moiety (*cis*); if this value is close to 180°, the orientation is anti-coplanar (*trans*). Additionally,  $\xi$  is positive if the heteroatom is below the plane defined by uracil and negative otherwise. In the presence of PAR, the selenophene ring shows mainly a conformation similar to the *cis* conformation, almost coplanar with the uracil ring and with the heteroatom below the plane of uracil ( $\xi > 0^\circ$ ). On the contrary, if PAR is absent, the selenophene moiety has larger degrees of freedom and can rotate. Therefore, <sup>5e</sup>U adopts different conformations, many of which having Se outside of the plane of the uracil moiety. Our results clearly point out that PAR reduces the rotation of the selenophene around the bond C2'–C5 in <sup>5e</sup>U.

We also analyzed the hydrogen bonds of the uracil ring of <sup>5e</sup>U in these two situations (Figure S1). In the crystal structure of the modified rRNA, <sup>5e</sup>U forms two hydrogen bonds with the carbonyl oxygen and the amide hydrogen of U1495. These interactions are preserved in the absence of the antibiotic (–PAR, Figure S1). But as soon as the antibiotic is bound, <sup>5e</sup>U is shifted away from its initial position by about 4 Å due to the bulkiness of PAR, changing the interactions of <sup>5e</sup>U with U1495: now, the oxygen on C4 of <sup>5e</sup>U forms a hydrogen bond with the amide nitrogen of U1495. We also characterized the binding mode of PAR to the rRNA (Figure S2). The energy binding analysis shows that the main interactions of PAR are with G1491 and G1494 through several electrostatic interactions between the ammonium groups in PAR and the backbone and/or nucleobases of RNA (Figure S2). To sum up, the presence of PAR affects both the interactions of the nucleobase with its partners and the rotation around the C2'–C5 bond of the selenophene ring (aka. its relative orientation vs. uracil).

### Influence of paromomycin on the emission spectrum of <sup>5e</sup>U

Next, we computed the emission spectra under both circumstances (+PAR, –PAR) taking into account the dynamic behavior of the rRNA and its vibrational levels (Sections S2 and S3). We ran parallel QM/MM MD simulations on the first excited state ( $S_1$ ) of the nucleobase of <sup>5e</sup>U and incorporated in the rRNA. Compared to the computation of absorption spectra, now the propagation of the electronic wavefunction is done on the first excited state  $S_1$ . We selected BP86-D3/def2-SVP<sup>[21]</sup> for our simulations, and the Hamiltonian was polarized with the point charges of the environment. Selection of this functional was based on the comparison of the computed emission maximum of the nucleoside form of <sup>5e</sup>U in water with ADC(2)<sup>[22]</sup> as the theoretical method of reference ( $\Delta E = 0.18$  eV between the calculated emission maxima). In Figure 3 we

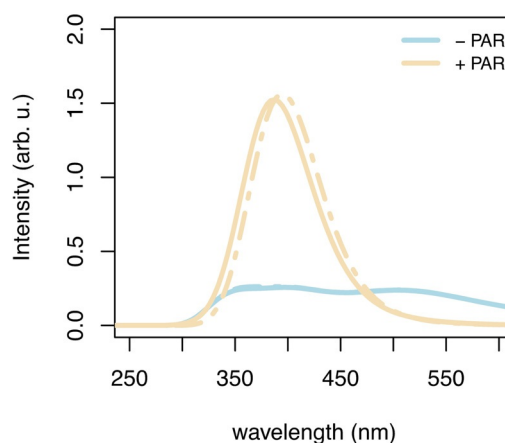


**Figure 3.** Computed emission spectra of <sup>5e</sup>U within rRNA in the absence (–PAR, light blue line) or in the presence (+PAR, wheat line) of paromomycin. Dotted lines represent the situation without point charges to represent the environment.

show the computed emission spectra in the presence (+PAR) and in the absence (–PAR) of the antibiotic. A total of 92 excited states were used to convolute each of the spectra. As a result, we found that the presence of PAR increases significantly the intensity of the emission of <sup>5e</sup>U.

Having reproduced the experimental behavior previously evidenced by Srivatsan et al.,<sup>[14]</sup> we were committed to find out which was the main factor responsible for the increase of the fluorescence of <sup>5e</sup>U in the presence of PAR: the interactions with the solvent and/or interactions with the partners during the emission process (solvatochromic effect), or the relative orientation of the two rings of the fluorophore in <sup>5e</sup>U (structural effect)?

To answer these questions, we first evaluated the effect of the environment on the emission of the probe. If the increase of the fluorescence in <sup>5e</sup>U were due to interactions with the environment during the emission process, the spectra in both situations (+PAR, –PAR) would be similar if the electrostatic interactions with the media were removed. Thus, we computed the emission spectra of both systems again, keeping the geometries of the fluorophore, but in this case, removing any charge of the environment (+PAR/–PAR, dotted lines in Figure 3). We found out a smooth effect on the emission of the probe in both cases. These data confirmed that the relative conformation of fluorophore in <sup>5e</sup>U could determine the emissive properties of the probe. Of course, the environment affects which of those conformations are populated but its electrostatic effect on the emission seems not so relevant.

### Emission depends on the orientation of the selenophene ring

Based on the former findings, we looked at the dependence of the intensity of the emission (using as variable the oscillator strength of the  $S_1$  states) on the dihedral angle  $\xi$ —which gives us the relative orientation of the two rings in the fluorophore—defined in Figure 1 at all wavelength values. Previous theoretical studies have shown that two-ring fluorophore con-

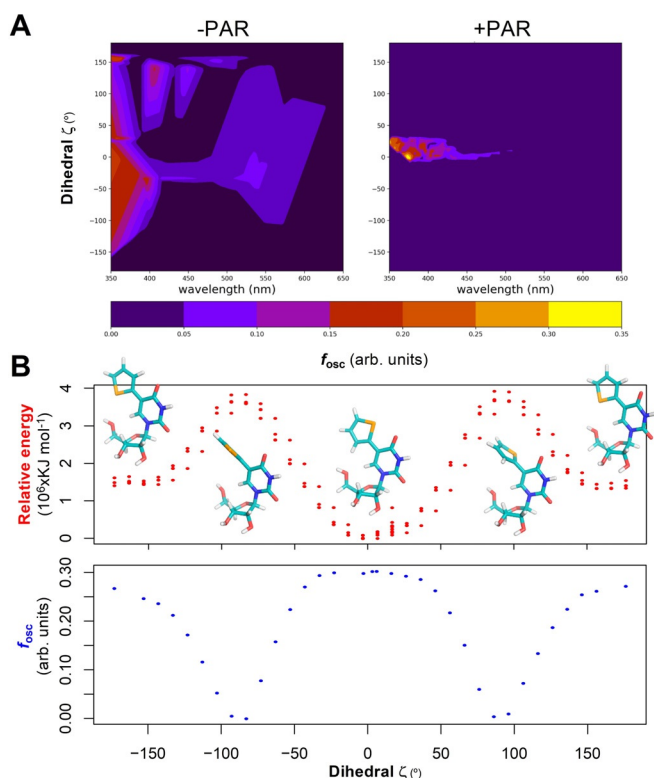


**Figure 4.** A) Correlation between emission wavelength [nm], dihedral angle  $\xi$  [degree] and oscillator strength for -PAR and +PAR. B) Energy scan [kJ mol<sup>-1</sup>] of  $\xi$  [degree] around the C2''-C5 bond and oscillator strength ( $f_{osc}$ ) calculated for some conformers.

nected to 2'-deoxycytidine tend to adopt a co-planar conformation when propagating on the  $S_1$  excited state.<sup>[23]</sup> As can be seen in Figure 4A, in the absence of PAR, <sup>5e</sup>U populates conformations with different values of  $\xi$ . Of these conformations, those close to 0° (*cis*) are the more emissive ones and those close to a value of  $\pm 90^\circ$  for the dihedral angle, are barely emissive. These states show stronger emission. This confirms that emission depends on  $\xi$ . In the presence of PAR, the conformational space of <sup>5e</sup>U is restricted to positive values of  $\xi$  around 0°. Complementarily, we did a dihedral scan around the C2''-C5 bond in implicit solvent (water) and we computed the brightness of the  $S_1$  excited state at certain points (Figure 4B). In line with our results in the RNA context, the in-plane conformations of the two rings (0°,  $\pm 180^\circ$ ) are the brightest conformations. These correspond also to the minima in the energy surface of the ground state. In contrast, the out-of-plane conformations ( $\pm 90^\circ$ ) are darker in particular for the perpendicular disposition of both rings ( $\xi = 90^\circ$ ).

### Excited states analysis

Finally, we analyzed the excited states of the probe under different circumstances. In Figure 5A are plotted the relevant molecular orbitals implicated in the fluorescence phenomenon: from  $S_1$  to  $S_0$ . Upon deexcitation, the excited electron, which was mainly localized on the uracil ring, "comes back" to the  $\pi$ -system on the selenophene ring. In these two rings are mainly

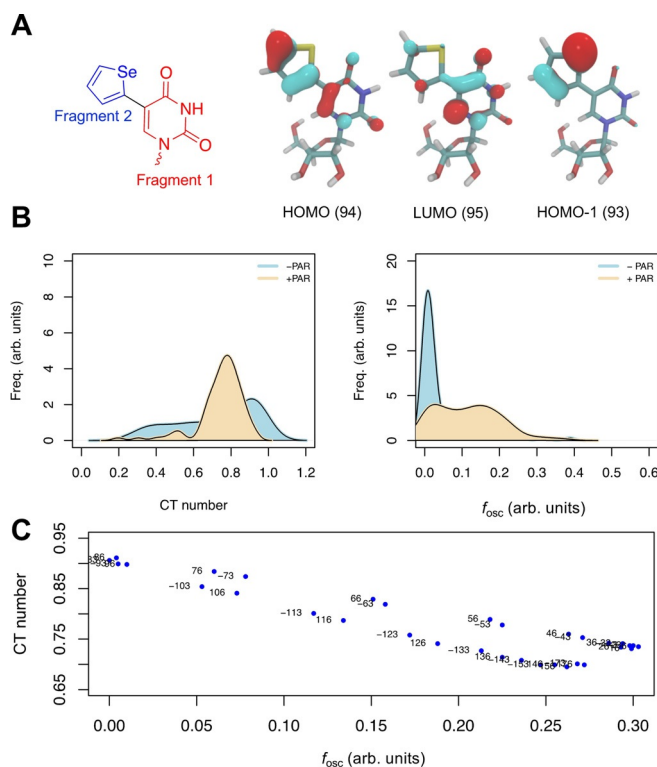


**Figure 5.** A) Definition of fragments and frontier molecular orbitals implicated in the  $S_1 \rightarrow S_0$  electronic de-excitation in <sup>5e</sup>U. Kohn–Sham orbitals computed by using the optimized geometry on the  $S_1$  energy surface (isovalue = 0.05). B) Distribution of the CT number (left) and oscillator strength (right) values of <sup>5e</sup>U along the excited state QM/MM MD simulations. C) CT number and  $f_{osc}$  for different geometries along the scan of dihedral  $\xi$  (dihedral angle values are given on each point).

located the LUMO and the HOMO, respectively. Therefore, we analyzed the transition density matrix of the system by dividing the fluorophore in two fragments:<sup>[24]</sup> the uracil moiety and the selenophene part. Doing this, we traced the charge transfer (CT) number between both fragments. A third fragment was defined for the sugar moiety but no relevant contribution to the fluorescence was found. In Figure 5B are plotted the distributions of CT numbers and oscillator strengths for both systems. In all cases, there is a strong CT component between the uracil and the selenophene moieties, with most of the states with CT character  $\geq 0.7$ .

Nevertheless, there are deep differences in the oscillator strength values of +PAR and -PAR. We also measured the CT number and oscillator strength during the dihedral scan of  $\xi$  (Figure 5C). There is a negative linear correlation between CT and  $f_{osc}$  (Pearson correlation coefficient = -0.92, 95% confidence interval). The darkest states ( $f_{osc} \rightarrow 0$ ), which correspond to  $\xi = \pm 90^\circ$ , show CT numbers  $\geq 0.9$  and the brightest states ( $\xi = 0, \pm 180^\circ$ ) reduce their CT to  $\approx 0.7$ . These differences on the CT numbers can be ascribed to the participation of the HOMO-1 in the deexcitation from  $S_1 \rightarrow S_0$ , which is exclusively located on the selenophene ring. The former molecular orbital corresponds to the  $\pi_2$  orbital of the heterocycle.<sup>[25]</sup> This molecular orbital has a strong contribution of the  $n$  electrons of the Se atom as shown in Figure 5A. Its contribution is relevant

when  $\xi = \pm 90^\circ$ , what turns  $S_1$  into dark state due to a  $n\pi^*$  electronic transition, which usually does not emit in nucleobases.<sup>[26,27]</sup> The system will be trapped for a longer time on this dark  $S_1$  and it will need more time to relax, and possibly, via nonradiative mechanisms. This fact could open new possibilities of exploring the use of  $^5\text{eU}$  as photoreactive probes because i)  $^5\text{eU}$  is able to absorb enough energy in the range of  $\approx 4$  eV (brightest state  $S_5$  in our calculations) and ii) rotation around the C2'–C5 bond can be restrained, for example, by chemical modification of the adjacent positions to the former bond with bulky groups.

## Conclusions

We have quantified in this work that the turn-on effect in the fluorescence of  $^5\text{eU}$  in the presence of PAR is mainly caused by the retention of in-plane conformations of both rings of the nucleobase in  $^5\text{eU}$  and not due to changes in the polarity of the environment during the emission process. Therefore, the effect of the environment on the emission is manifest in the preferential population of certain conformers of the fluorophore. Thus, our approach strongly indicates that, with the availability of current computational tools, paying attention to the dynamics of the fluorophore in the context of the macromolecule (i.e., rRNA + antibiotic + solvent) should be taken as a general practice before computing fluorescence. Even more, exploration of the “dark conformations” of  $^5\text{eU}$  could lead to future families of photoreactive probes.

## Acknowledgements

N.R.-B. thanks Xunta de Galicia for a postdoctoral grant and also for financial support through project GRC2019/24. We thank the research group of Prof. Leticia González (University of Vienna) for computational support.

## Conflict of Interests

The authors declare no conflict of interests.

**Keywords:** antibiotics · excited states · fluorescence probes · QM/MM · RNA

- [1] B. D. Davies, J. Davis, *J. Biol. Chem.* **1968**, *243*, 3312–3316.
- [2] D. N. Wilson, V. Hauryliuk, G. C. Atkinson, A. J. O'Neill, *Nat. Rev. Microbiol.* **2020**, *18*, 637–648.
- [3] J. M. A. Blair, M. A. Webber, A. J. Baylay, D. O. Ogbolu, L. J. V. Piddock, *Nat. Rev. Microbiol.* **2015**, *13*, 42–51.
- [4] R. E. Schroeder, C. Waldsich, H. Wank, *EMBO J.* **2000**, *19*, 1–9.
- [5] A. P. Carter, W. M. Clemons, D. E. Brodersen, R. J. Morgan-Warren, B. T. Wimberly, V. Ramakrishnan, *Nature* **2000**, *407*, 340–348.
- [6] B. S. Morgan, J. E. Forte, A. E. Hargrove, *Nucleic Acids Res.* **2018**, *46*, 8025–8037.
- [7] H. Kobayashi, M. Ogawa, R. Alford, P. L. Choyke, Y. Urano, *Chem. Rev.* **2010**, *110*, 2620–2640.
- [8] B. Llano-Sotelo, R. P. Hickerson, L. Lancaster, H. F. Noller, A. S. Mankin, *Rna* **2009**, *15*, 1597–1604.
- [9] M. Kaul, C. M. Barbieri, D. S. Pilch, *J. Am. Chem. Soc.* **2004**, *126*, 3447–3453.
- [10] C. Cao, P. Wei, R. Li, Y. Zhong, X. Li, F. Xue, Y. Shi, T. Yi, *ACS Sens.* **2019**, *4*, 1409–1416.
- [11] W. Xu, K. M. Chan, E. T. Kool, *Nat. Chem.* **2017**, *9*, 1043–1055.
- [12] A. León Buitimea, C. R. Garza-Cárdenas, J. A. Garza-Cervantes, J. A. Lerma-Escalera, J. R. Morones-Ramírez, *Front. Microbiol.* **2020**, *11*, 1–10.
- [13] M. G. Pawar, A. Nuthanakanti, S. G. Srivatsan, *Bioconjugate Chem.* **2013**, *24*, 1367–1377.
- [14] A. Nuthanakanti, M. A. Boerneke, T. Hermann, S. G. Srivatsan, *Angew. Chem. Int. Ed.* **2017**, *56*, 2640–2644; *Angew. Chem.* **2017**, *129*, 2684–2688.
- [15] A. Rozov, E. Westhof, M. Yusupov, G. Yusupova, *Nucleic Acids Res.* **2016**, *44*, 6434–6441.
- [16] I. Prokhorova, R. B. Altman, M. Djumagulov, J. P. Shrestha, A. Urzhumtsev, A. Ferguson, C. W. T. Chang, M. Yusupov, S. C. Blanchard, G. Yusupova, *Proc. Natl. Acad. Sci. USA* **2017**, *114*, E10899–E10908.
- [17] Q. Vicens, E. Westhof, *Structure* **2001**, *9*, 647–658.
- [18] D. Fourmy, M. I. Recht, S. C. Blanchard, J. D. Puglisi, *Science* **1996**, *274*, 1367–1371.
- [19] M.-P. Mingeot-Leclercq, Y. Glupczynski, P. M. Tulkens, *Antimicrob. Agents Chemother.* **1999**, *43*, 727–737.
- [20] Q. Vicens, E. Westhof, *Chem. Biol.* **2002**, *9*, 747–755.
- [21] F. Weigend, R. Ahlrichs, *Phys. Chem. Chem. Phys.* **2005**, *7*, 3297–3305.
- [22] J. Schirmer, *Phys. Rev. A* **1982**, *26*, 2395–2416.
- [23] J. Stendevad, M. Hornum, D. Wüstner, J. Kongsted, *Photochem. Photobiol. Sci.* **2019**, *18*, 1858–1865.
- [24] F. Plasser, *J. Chem. Phys.* **2020**, *152*, 084108.
- [25] A. Prlj, B. F. E. Curchod, C. Corminboeuf, *Phys. Chem. Chem. Phys.* **2015**, *17*, 14719–14730.
- [26] Y. Mercier, F. Santoro, M. Reguero, R. Improta, *J. Phys. Chem. B* **2008**, *112*, 10769–10772.
- [27] K. E. Szkaradek, P. Stadlbauer, J. Šponer, R. W. Góra, R. Szabla, *Chem. Commun.* **2020**, *56*, 201–204.

Manuscript received: November 3, 2020

Accepted manuscript online: December 23, 2020

Version of record online: February 8, 2021